AD-A062 070 RAYTHEON CO SUDBURY MASS EQUIPMENT DIV F/G 20/5
LASER DOPPLER RADAR SYSTEM CALIBRATION AND RAINFALL ATTENUATION--ETC(U)
OCT 78 DOT-TSC-1218

UNCLASSIFIED ER78-4018 FAA/RD-78/40 NL

1 OF 1
AD A062 070

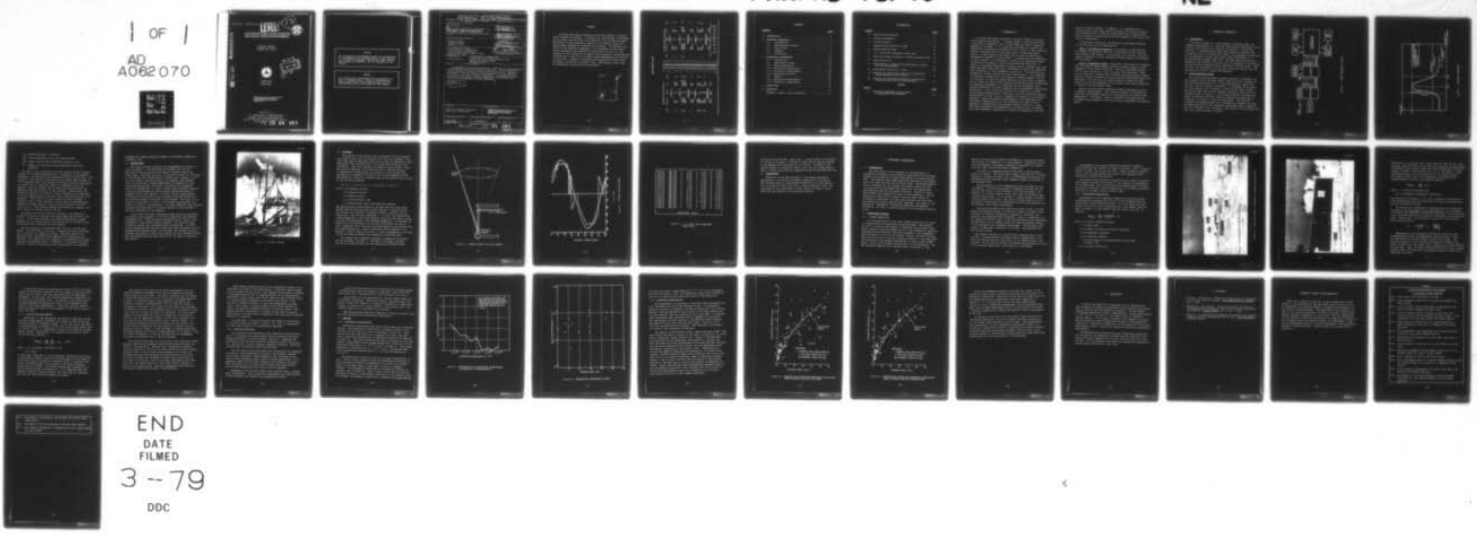

END
DATE FILMED
3-79
DDC

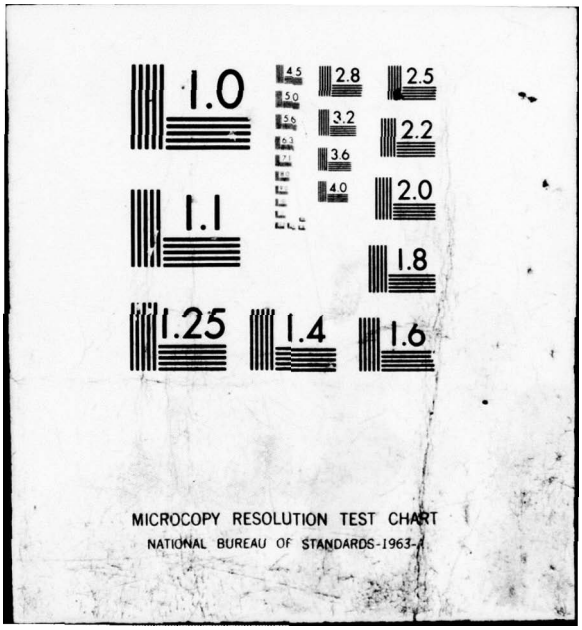
1.0
1.1
1.25
1.4
1.6
1.8
2.0
2.2
2.5
2.8
3.2
3.6
4.0
4.5
5.0
5.6
MICROCOPY RESOLUTION TEST CHART
NATIONAL BUREAU OF STANDARDS-1963-A

REPORT NO. FAA-RD-78-40

LEVEL II (13)

LASER DOPPLER RADAR SYSTEM CALIBRATION AND RAINFALL ATTENUATION MEASUREMENTS

Raytheon Company
Equipment Division
Sudbury MA 01776

OCTOBER 1978

FINAL REPORT

Prepared for

U.S. DEPARTMENT OF TRANSPORTATION
FEDERAL AVIATION ADMINISTRATION
Systems Research and Development Service
Washington DC 20590

NOTICE

This document is disseminated under the sponsorship of the Department of Transportation in the interest of information exchange. The United States Government assumes no liability for its contents or use thereof.

NOTICE

The United States Government does not endorse products or manufacturers. Trade or manufacturers' names appear herein solely because they are considered essential to the object of this report.

(18) FAA/RD, TSC (19) 78/40, FAA-78-8

Technical Report Documentation Page

1. Report No.	2. Government Accession No.	3. Recipient's Catalog No.
FAA-RD-78-40		

4. Title and Subtitle	5. Report Date
(6) LASER DOPPLER RADAR SYSTEM CALIBRATION AND RAINFALL ATTENUATION MEASUREMENTS	(11) October 1978
	6. Performing Organization Code
7. Author's	8. Performing Organization Report No. (14) ER78-4018 Raytheon # DOT-TSC-FAA-78-8

9. Performing Organization Name and Address	10. Work Unit No. (TRAIS)
Raytheon Company* Equipment Division Sudbury MA 01776	FA842/R8105
	11. Contract or Grant No. (15) DOT-TSC-1218

12. Sponsoring Agency Name and Address	13. Type of Report and Period Covered
U.S. Department of Transportation Federal Aviation Administration Systems Research and Development Service Washington DC 20590	(9) Final Report June 1976 - Dec. 1977
	14. Sponsoring Agency Code

15. Supplementary Notes

*Under contract to: U.S. Department of Transportation
Research and Special Programs Administration
Transportation Systems Center
Cambridge MA 02142

16. Abstract

The atmospheric attenuation and backscatter coefficients have been measured at the 10.6-micrometers wavelength of the CO_2 laser in rainstorms. Data are presented to show the increase in attenuation coefficient with rainfall rate. Backscatter coefficients in rain and clear air are also presented. Data were collected on a 460-meter test range at Sudbury, Massachusetts. The experimental results can be used to evaluate the performance capabilities of CO_2 coherent laser systems for making atmospheric velocity measurements.

(12) 41 p.

17. Key Words	18. Distribution Statement
Carbon Dioxide Laser, Attenuation, Backscatter, Rainfall Rate	DOCUMENT IS AVAILABLE TO THE U.S. PUBLIC THROUGH THE NATIONAL TECHNICAL INFORMATION SERVICE, SPRINGFIELD, VIRGINIA 22161

19. Security Classif. (of this report)	20. Security Classif. (of this page)	21. No. of Pages	22. Price
Unclassified	Unclassified	40	

Form DOT F 1700.7 (8-72) Reproduction of completed page authorized

405 037 78 12 04 161

PREFACE

Low-level wind shear represents a potential hazard to aircraft during takeoff and landing. A coherent CO_2 laser-Doppler velocimeter may be useful for monitoring this condition, and it would be highly desirable for such a system to operate in all-weather conditions during which takeoffs and landings are permitted. To determine the extent of the systems's capability, it is necessary to know atmospheric backscatter and attenuation coefficients at 10.6 μm. The purposes of this study were to measure the attenuation and backscatter coefficients in rain and to correlate these measurements with meteorological data. Graphs of attenuation and backscatter coefficients are shown as functions of rainfall rate. Additionally, some clear air backscatter coefficients are presented.

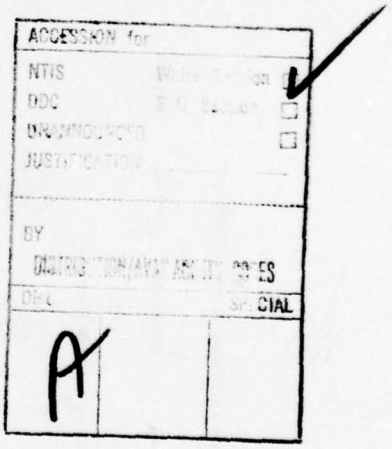

METRIC CONVERSION FACTORS

Approximate Conversions to Metric Measures

Symbol	When You Know	Multiply by	To Find	Symbol
		LENGTH		
in	inches	2.5	centimeters	cm
ft	feet	30	centimeters	cm
yd	yards	0.9	meters	m
mi	miles	1.6	kilometers	km
		AREA		
in^2	square inches	6.5	square centimeters	cm^2
ft^2	square feet	0.09	square meters	m^2
yd^2	square yards	0.8	square meters	m^2
mi^2	square miles	2.6	square kilometers	km^2
	acres	0.4	hectares	ha
		MASS (weight)		
oz	ounces	28	grams	g
lb	pounds	0.45	kilograms	kg
	short tons (2000 lb)	0.9	tonnes	t
		VOLUME		
tsp	teaspoons	5	milliliters	ml
Tbsp	tablespoons	15	milliliters	ml
fl oz	fluid ounces	30	milliliters	ml
c	cups	0.24	liters	l
pt	pints	0.47	liters	l
qt	quarts	0.95	liters	l
gal	gallons	3.8	liters	l
ft^3	cubic feet	0.03	cubic meters	m^3
yd^3	cubic yards	0.76	cubic meters	m^3
		TEMPERATURE (exact)		
°F	Fahrenheit temperature	5/9 (after subtracting 32)	Celsius temperature	°C

Approximate Conversions from Metric Measures

Symbol	When You Know	Multiply by	To Find	Symbol
		LENGTH		
mm	millimeters	0.04	inches	in
cm	centimeters	0.4	inches	in
m	meters	3.3	feet	ft
m	meters	1.1	yards	yd
km	kilometers	0.6	miles	mi
		AREA		
cm^2	square centimeters	0.16	square inches	in^2
m^2	square meters	1.2	square yards	yd^2
km^2	square kilometers	0.4	square miles	mi^2
ha	hectares (10,000 m^2)	2.5	acres	
		MASS (weight)		
g	grams	0.035	ounces	oz
kg	kilograms	2.2	pounds	lb
t	tonnes (1000 kg)	1.1	short tons	
		VOLUME		
ml	milliliters	0.03	fluid ounces	fl oz
l	liters	2.1	pints	pt
l	liters	1.06	quarts	qt
l	liters	0.26	gallons	gal
m^3	cubic meters	35	cubic feet	ft^3
m^3	cubic meters	1.3	cubic yards	yd^3
		TEMPERATURE (exact)		
°C	Celsius temperature	9/5 (then add 32)	Fahrenheit temperature	°F

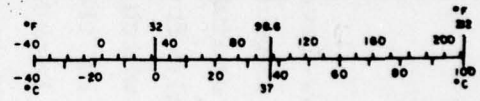

CONTENTS

ILLUSTRATIONS

TABLES

1. INTRODUCTION

Low level wind shear represents a potential hazard to aircraft during takeoff and landing. A sudden change in wind direction when an aircraft is operating close to stall speed can lead to dangerous changes in air speed. It is, therefore, desirable to consider the possibility of developing a system to alert a pilot to such conditions, thereby, providing him with the opportunity to take appropriate action. A laser Doppler velocimeter may be useful for making the measurements required for this system. In determining the feasibility of such a system, it is necessary to evaluate the operational characteristics of the system in various meteorological conditions. A number of successful measurement programs utilizing coherent CO_2 laser radar have shown that this type of instrument is useful for measuring wind velocities in clear atmospheric conditions. In determining the feasibility of such a system as a wind shear monitor, it is necessary to evaluate the capability of the system in adverse weather, such as rain and fog. It would be highly desirable for the system to operate in all conditions during which takeoffs and landings would be permitted. The important parameters to be measured are the atmospheric backscatter coefficient for laser radiation and the atmospheric attenuation coefficient. Both of these coefficients are expected to increase during adverse meteorological conditions, with the increases generally taking place in such a way as to degrade the operation of the system. Therefore, under this program, measurements of the backscatter and attenuation characteristics of the atmosphere were made, with an emphasis on measurements during adverse weather conditions. These data were correlated with measurements of rainfall rate, visibility, and other atmospheric parameters to assess the capability of the LDV

system in adverse weather. In addition, in a separate task, a surface-acoustic-wave (SAW) spectrum analyzer and digital processor were integrated into an existing laser radar with a complete data-analysis system for demonstrating the LDV capability for making wind-velocity measurements.

To meet these objectives, the program was performed according to the following two task descriptions:

Task 1. Processor Integration. An existing surface-acoustic-wave delay-line processor shall be incorporated into the existing laser-Doppler radar system. The processor will include a real-time computer capability and the necessary software package for assessing wind conditions.

Task 2. Atmospheric Tests. Calibration tests shall be conducted with the improved laser-Doppler system at suitable ranges to allow assessment of the system efficiency. Multiple calibrated targets will be used including at least one remote wind anemometer. Data will be collected, analyzed, and evaluated using the improved system during a variety of weather and wind conditions experienced during the test phase. The data will be compiled against a prescribed data format to allow the assessment of a low-power laser-system capability to operate in an all-weather mode.

The work was performed at Raytheon Company, Equipment Division, in Sudbury, Massachusetts. This facility includes a 500-meter test range and a considerable amount of instrumentation for making laser measurements. In addition, several instruments furnished by the Government were deployed on this test range to supplement the measurements.

2. PROCESSOR INTEGRATION

2.1 INTRODUCTION

An important aspect of a laser-Doppler velocimeter (LDV) for windshear measurements is a real-time data-analysis capability for determining wind velocity as a function of position. To meet this objective, a surface-acoustic-wave (SAW) delay-line processor was incorporated into the existing LDV system. The necessary interfacing was accomplished to permit the system to make measurements in a velocity-azimuth-display (VAD) mode. The data from each scan were analysed by the processor and input to a mini-computer for processing, and results were displayed before completion of the next scan. Additionally, the electronic circuitry for a simulated conical scan was developed as an aid for design and debugging.

2.2 DATA-PROCESSING SYSTEM

The existing data-processing system consisted of a Raytheon 706 mini-computer with 16,000-word memory, Tektronix 4010-1 display and the associated hard-copy unit, a time-code generator, paper-tape facility, and the required interfacing. To integrate the processor into this system it was necessary to enter the processor outputs and conical scan data into the computer interface. This was accomplished as shown in Figure 1. The spectrum analyzer processes the signal received by the laser system to determine the amplitude as a function of frequency of the received signal. The processor integrates the spectral data for a variable-time interval, provides for amplitude and velocity thresholds, and allows width integration; that is, integration over frequency. The outputs of the processor are four 8-bit words as shown in Figure 2;

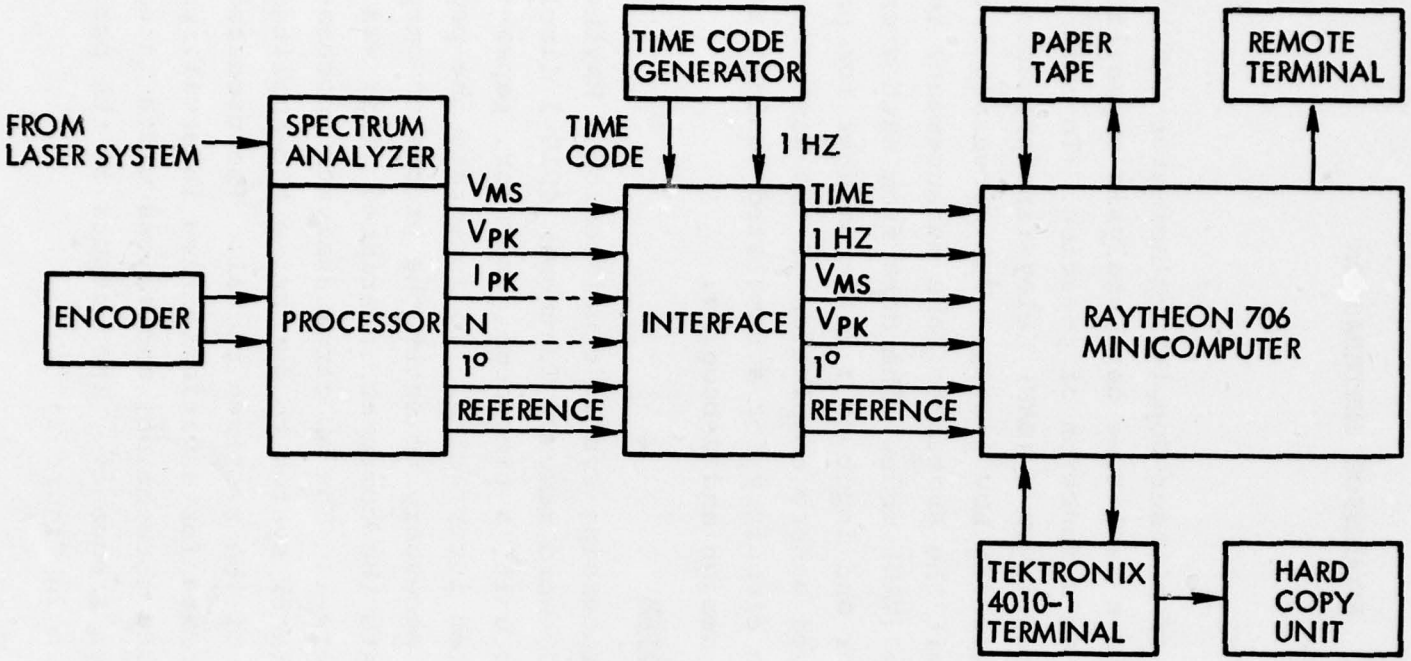

Figure 1. DATA-PROCESSING SYSTEM

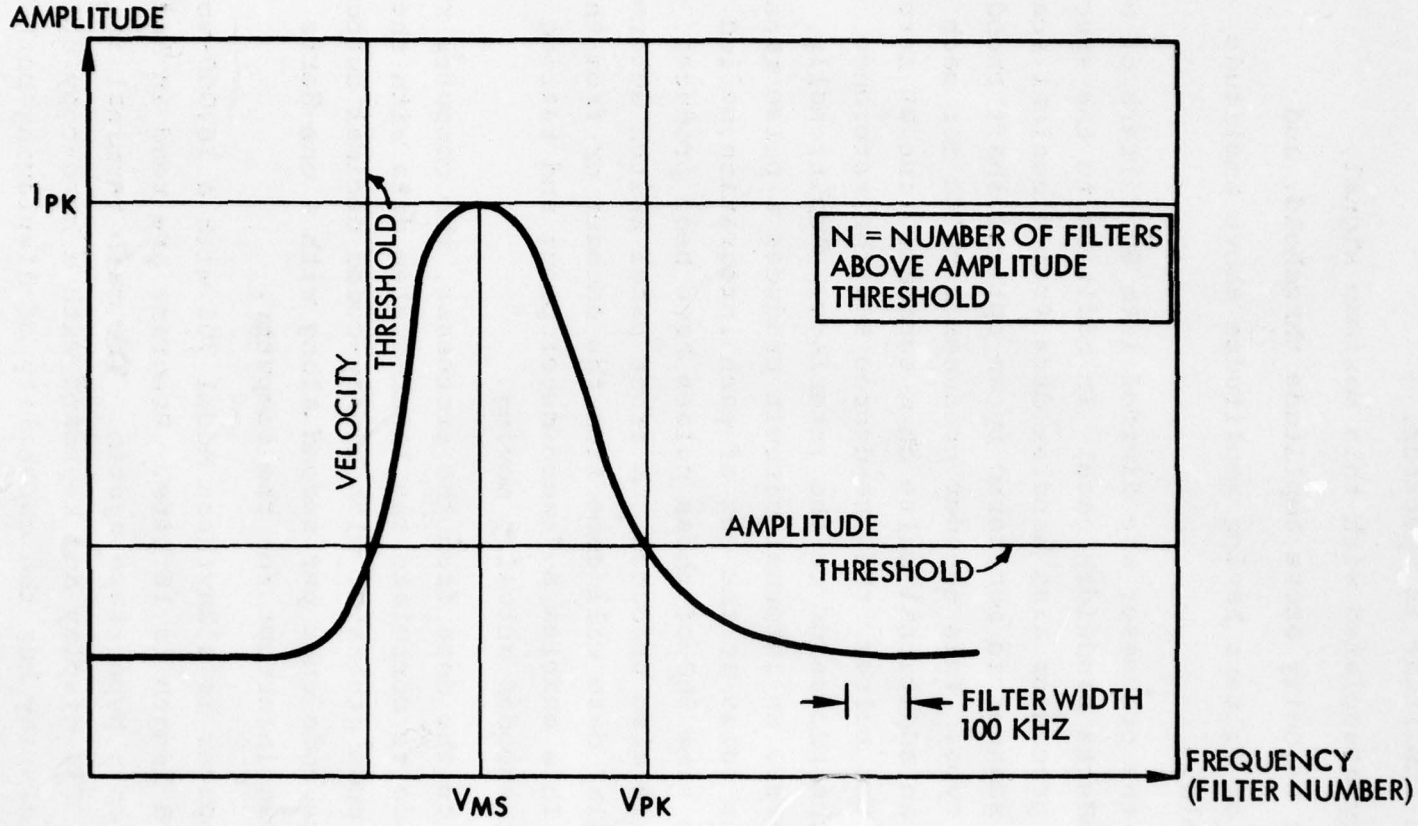

Figure 2. SPECTRAL PARAMETERS

I_{pk}, highest amplitude in spectrum,

V_{ms}, velocity associated with this maximum signal,

V_{pk}, highest velocity above amplitude threshold, and

N, number of filters having amplitudes above amplitude threshold.

The data in the processor are divided into 80 filters of approximately 100-kiloHertz bandwidth each. In addition to the spectral parameters, the processor also handles data from a conical scan. The position of the scanner is monitored by an optical shaft encoder of the incremental type. This encoder produces a pulse for each degree of rotation and an additional pulse on a separate line at zero degrees. These two pulses, the one-degree and the reference, are passed through the processor to the interface. Additionally, for diagnostic purposes, an internal circuit produces a pulse identical to the one-degree pulse at the end of each integration period of the processor. Each time 360 of these pulses have been produced, a reference pulse is also produced. A front panel switch determines whether the angular data will come from the encoder or from the local circuit. This enables software development and testing to be done without the encoder actually moving.

In addition to the data from the processor, the computer requires a time code to correlate the laser-system data with the time of day. A time code generator with binary-coded decimal outputs produces the time code once per second along with a one-Hertz pulse which serves as an interrupt for the computer.

The mini-computer is a Raytheon Model 706 with a 16,000-word memory. The word length is 16 bits. Programs are read in and data may be read out on a paper-tape system. The maib terminal is a Tektronix 4010-1 CRT display and keyboard with a hard-copy unit attached. This display has the capability of displaying both alphanumerical and graphical data. In addition, the provision is available for a remote terminal which may be hard-wired to the system or

operated at a remote location by means of an acoustic coupler and telephone lines.

2.3 CONICAL SCAN

The conical scanner consists of an arrangement of mirrors as shown in Figure 3. The laser beam is incident from the left hand side on the top mirror which bends it downward toward the lower mirror. The lower mirror is inclined at an angle of 15 degrees to the vertical and rotates about a vertical axis, producing a conical scan having a cone half angle of 30 degrees. The scanning mirror is driven by a variable speed motor at speeds up to three revolutions per second. The shaft of the motor is attached by means of a toothed belt to a shaft encoder which optically generates a pulse for each degree of rotation and an additional pulse on a separate line at zero degrees. In setting up the conical scanner, the scanner is positioned so that the beam is pointed toward the north and the encoder is aligned to zero degrees. The output of the encoder is connected to a pair of line drivers which generate the signal to be sent to the processor. In normal operation, the processor transmits the pulses from the encoder directly to the interface to serve as interrupts for the computer.

In the local scan mode, simulated encoder pulses are generated internally in the processor to be used in diagnostic and algorithm development work. These pulses are generated by the timing of the integration in the digital signal processor. At the end of each integration period, the one-degree pulse is generated. A counter circuit determines when 360 such pulses have been generated, and also generates the reference pulse. In this way, the internal circuitry imitates the function of the conical scanner so that software development and debugging may be performed without the need for operating the scanner.

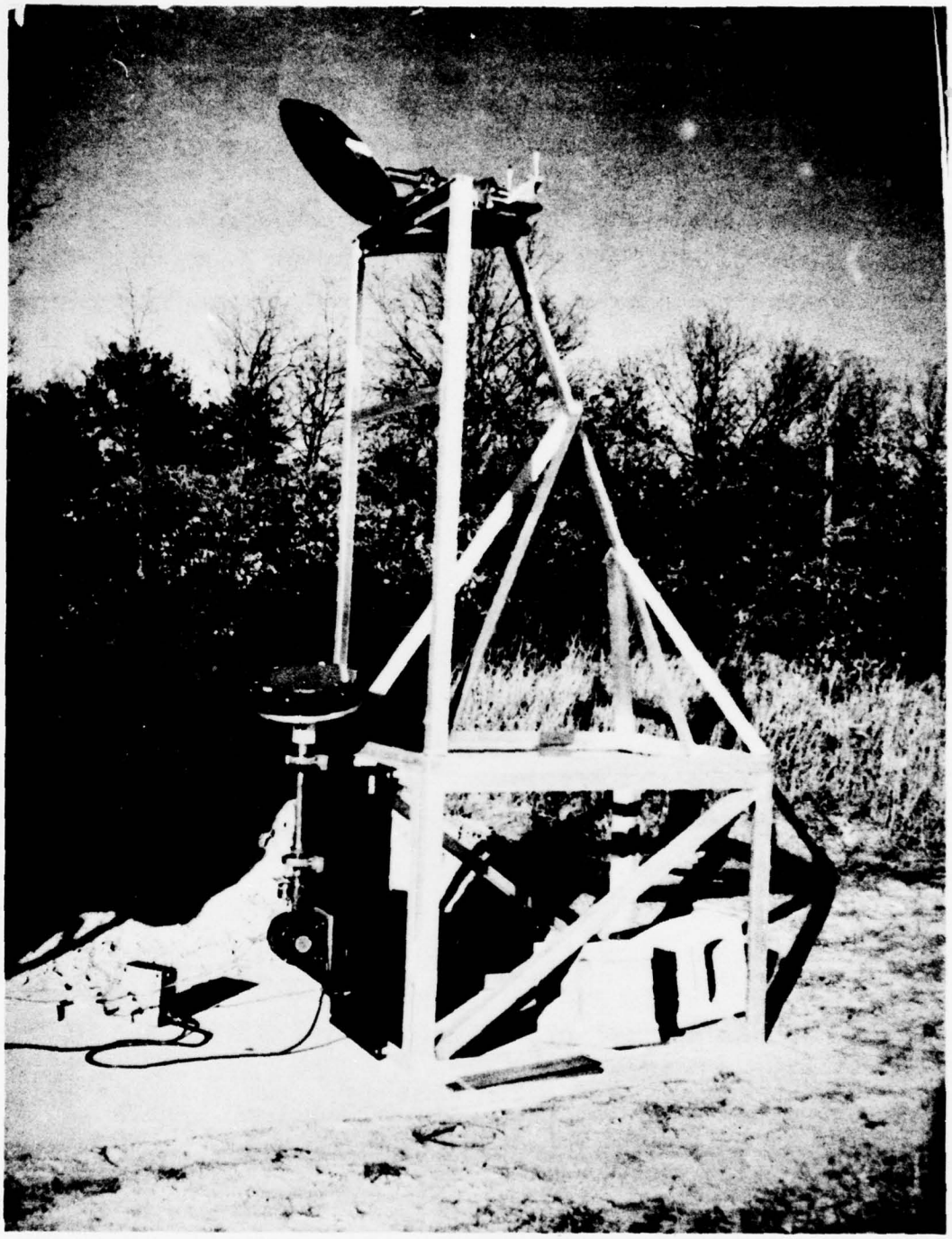

Figure 3. CONICAL SCANNER

2.4 SOFTWARE

The purpose of the software for the Raytheon 706 mini-computer is to read in data from the processor and time code generator, display these data in meaningful form, use the data to calculate a three-dimensional wind velocity vector, and output the results of this calculation. The first function is display of the raw data. These data may be displayed on the Tektronix 4010-1 display tabularly, or graphically to demonstrate the operation of the conical scan. Considering the diagram in Figure 4, the velocity measured by the LDV system as a function of azimuth angle of the conical scan is given by the following equation;

$$V_{||}(\theta) = | u \cos\theta \sin\delta + v \sin\theta \sin\delta + w \cos\delta | ,$$

where u is northward velocity,

v is westward velocity,

w is upward velocity,

δ is cone half-angle, and

θ is azimuth angle with north being zero degrees.

The absolute value arises because of the fact that the laser radar system does not sense the sign of the velocity. A typical plot of the velocity as a function of azimuth is shown in Figure 5 by the rough curve. The velocity components, u, v, and w, are obtained by a least-squares fit to the above equation using the data from a single scan with the components as the variable parameters. To evaluate the operation of the algorithm, the sine wave calculated from the u, v, and w components may be plotted on the same graph as the raw data with the reconstituted sign. This is the smooth curve referred to in Figure 5. Figure 6 shows a set of u, v, and w components as functions of time from data collected with successive single VAD scans.

The display most frequently employed in operating this system was the one shown in Figure 5. The axes of the graph are drawn and the two curves plotted; the raw data with the reconstituted

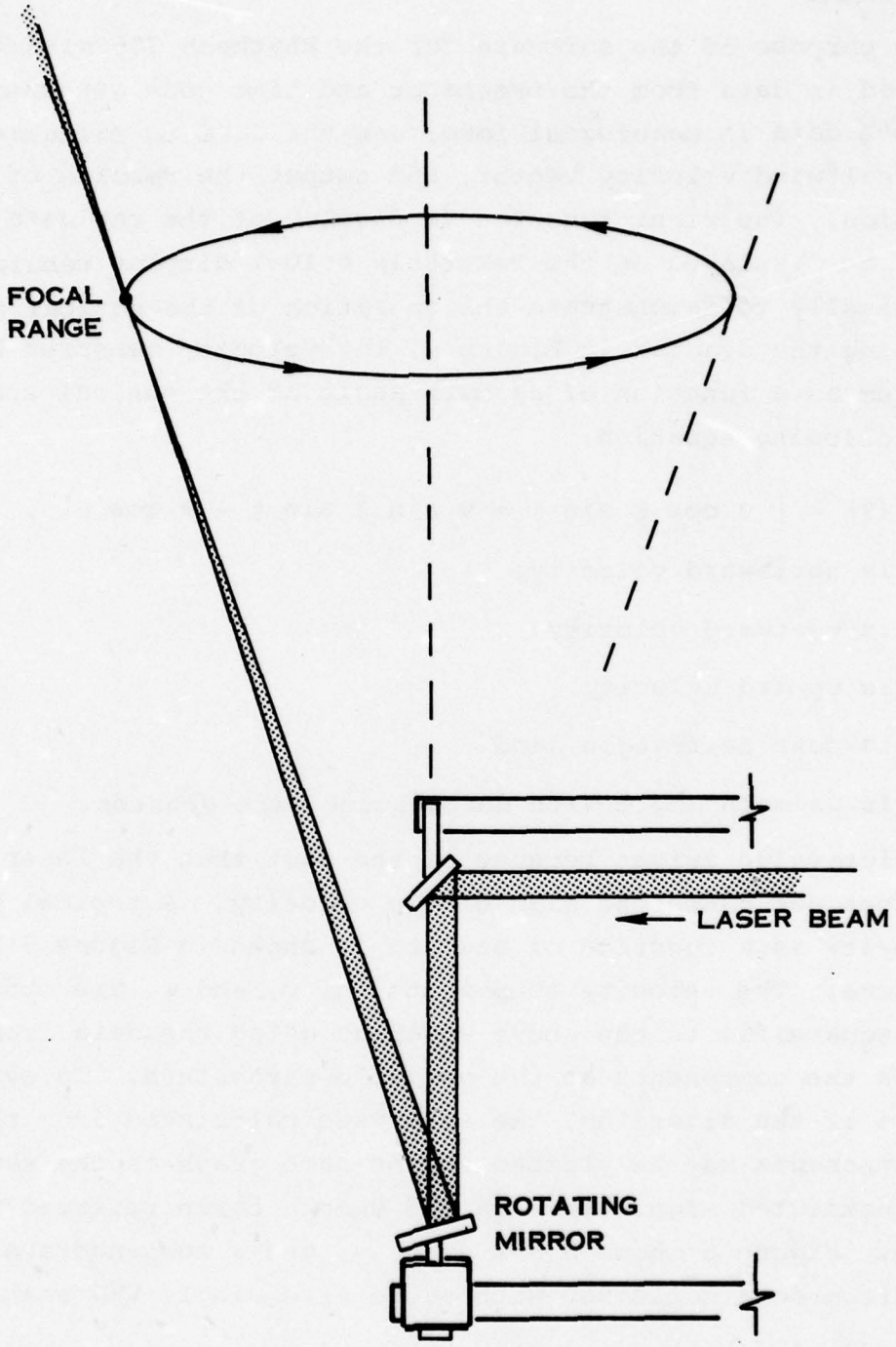

Figure 4. UPWARD-LOOKING VAD SCAN CONCEPT

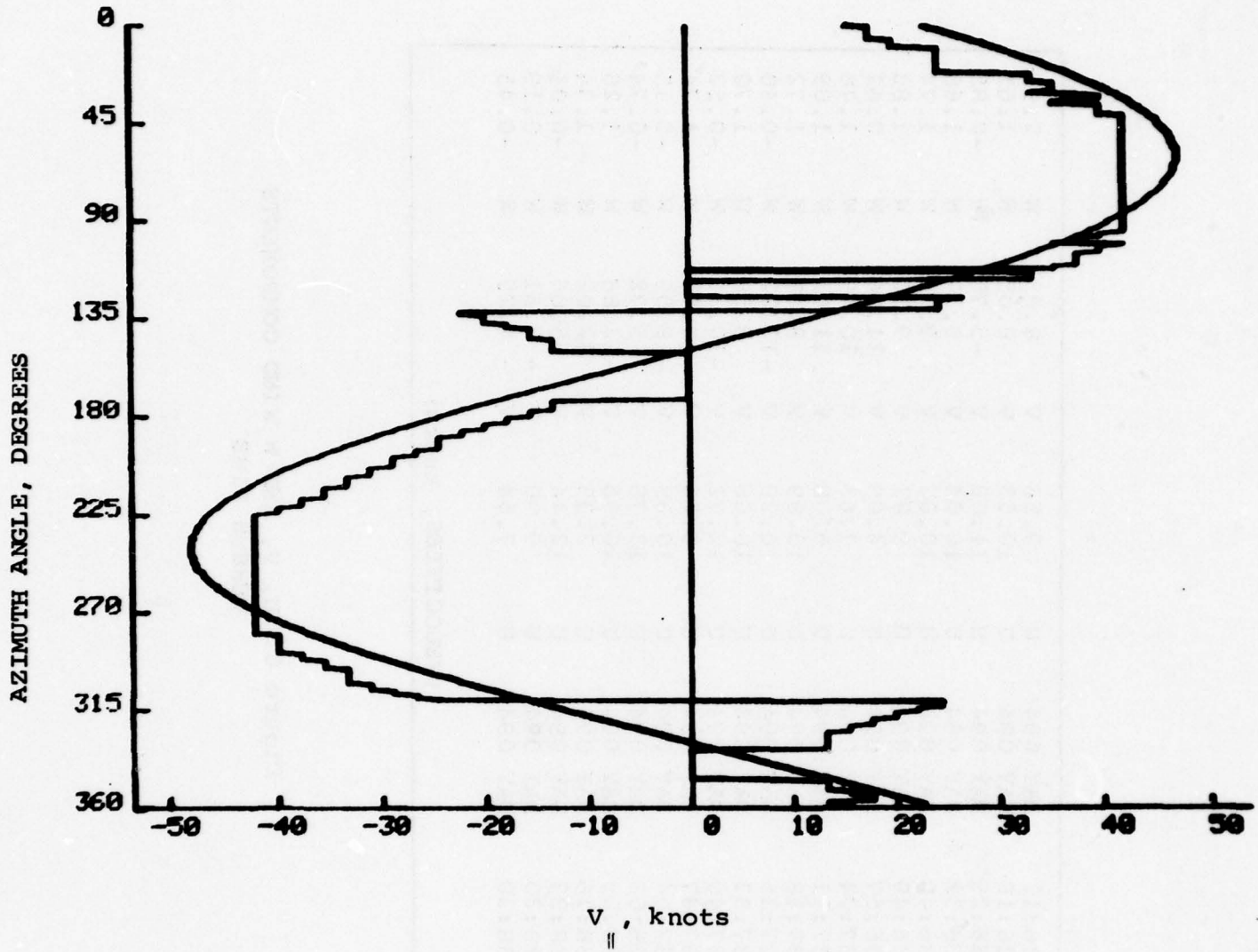

Figure 5. TYPICAL VAD SCAN DATA

1136:11	DAY 094	U	9.56	V	8.03	W	2.92
1136:18	DAY 094	U	10.53	V	8.05	W	1.61
1136:25	DAY 094	U	11.00	V	-5.78	W	-0.85
1136:32	DAY 094	U	10.04	V	9.37	W	1.68
1136:40	DAY 094	U	10.02	V	9.03	W	1.74
1136:49	DAY 094	U	9.81	V	9.30	W	1.83
1136:57	DAY 094	U	4.09	V	11.04	W	0.61
1137:04	DAY 094	U	7.63	V	10.49	W	1.46
1137:11	DAY 094	U	6.08	V	11.61	W	1.09
1137:18	DAY 094	U	10.89	V	8.43	W	1.72
1137:25	DAY 094	U	0.29	V	-12.23	W	-0.40
1137:33	DAY 094	U	10.68	V	8.58	W	1.70
1137:40	DAY 094	U	12.72	V	-10.36	W	-0.52
1137:47	DAY 094	U	9.26	V	10.02	W	1.74
1137:54	DAY 094	U	10.68	V	- 9.05	W	-0.15
1138:02	DAY 094	U	13.78	V	5.72	W	-0.74
1138:09	DAY 094	U	10.96	V	-12.88	W	1.26
1138:16	DAY 094	U	2.35	V	12.02	W	1.34
1138:23	DAY 094	U	12.44	V	5.06	W	-0.01
1138:30	DAY 094	U	9.90	V	- 8.81	W	0.19
1138:38	DAY 094	U	7.54	V	- 7.25	W	-0.45

(VELOCITIES, knots)

Figure 6. U, V, AND W WIND COMPONENTS VERSUS TIME

sign and the fitted data. Then, the u, v, and w results are printed at the top of the page. A variety of scale factors may be employed to accommodate wind velocities up to 50 knots. In addition, the remote terminal is frequently used to print only the final results; the u, v, and w wind velocity components along with the date and time.

2.5 CONCLUSIONS

Integration of the SAW processor to the system provided an improvement to the velocity processing capability of the system. The high-duty cycle of the processor resulted in an 11-dB improvement in signal-to-noise ratio with a 2-msec integration time. The usefulness of this improvement is most evident in Figure 5 which shows the high quality of velocity data obtained.

3. ATMOSPHERIC MEASUREMENTS

3.1 INTRODUCTION

The major effort on this program was the measurement of atmospheric backscatter and attenuation characteristics in adverse weather and correlation of these measurements with meteorological data. The existing laser-radar system was employed at the Sudbury laser test facility using the 500-meter range. Calibrated measurements of signals from two targets at different ranges and from one target and the atmosphere were made along with appropriate meteorological data for correlation purposes. Results of these measurements were compared with those in the references. Initial experimental difficulties produced unusually small values of attenuation coefficient, but when these problems were rectified, the attenuation values obtained were comparable with those in the references. Backscatter coefficients exhibited considerable variability, but were in general agreement with previously measured values.

3.2 MEASUREMENT PROGRAM

3.2.1 SYSTEM DESCRIPTION

A brief description of the laser Doppler system will be useful in understanding the measurements which were made. The coherent CO_2 LDV is a laser system capable of measuring line-of-sight atmospheric velocity using the Doppler shift in the frequency of radiation backscattered from aerosols naturally suspended in the atmosphere. Small particles in the air such as dust, pollen, and water droplets, that are moving with a velocity component parallel to the beam, shift the frequency of the backscattered photons an amount equal to $\frac{2v}{\lambda}$, where v is the line-of-sight velocity, and λ is the wavelength. The LDV processor measures this frequency shift, digitizes it, and

inputs it along with the spatial coordinates of the point at which the velocity was measured, to a mini-computer. Through the use of the mini-computer, the system is capable of operation at a remote site with real time data-processing capability.

The laser is a Raytheon model LS-10A with a nominal output power of 17 watts. The output beam is TEM_{oo} with the $1/e^2$ intensity points at a diameter of about 7 mm. The horizontal polarization is determined by Zinc Selenide (ZnSe) Brewster windows on the ends of the discharge tube.

The telescope is an f/8 Cassegrainian with a primary one foot in diameter. It serves the purpose of expanding the beam and controlling the range to focus by means of a moving secondary. The detector is a liquid-nitrogen cooled (77K) Lead Tin Telluride chip of about 250-μm width. It is mounted in a dewar capable of holding liquid nitrogen for 8 hours. The local oscillator power of a few milliwatts is sufficient to provide shot-noise-limited operation of the detector over 60 MHz of bandwidth.

The spectrum analyzer and spectrum processor consist of a SAW delay line spectrum analyzer followed by a digital processor which provides for temporal and spectral integration, amplitude, low-frequency and frequency-width thresholds, linear or logarithmic output ranges, and digital output of the selected spectrum and parameters. The SAW delay line is ideally suited for spectral analysis because of its high-duty-cycle frequency measurements. The processor bandwidth is 10 MHz with a resolution of 100 kHz. The amplitude has 256 discrete levels.

The scanner consists of a tilted mirror rotating about a vertical axis. The beam enters from above using a bending mirror, and then is reflected from the scan mirror at a 30 degree angle to the vertical. As the scanner rotates, the focused spot describes a circle in a horizontal plane above, and centered on, the system.

Photographs of the system installed at Raytheon's Sudbury Electro-Optical test facility are shown in Figures 7 and 8. Figure 7 shows an overall view of the test site. Figure 8 shows an external view of the van which permits the system to be completely self-supporting on remote-site missions.

The targets used consisted of abrasive belts mounted on electric-belt sanders inclined at 45 degrees to the direction of propagation of the laser beam. The belts were moved at approximately 15 meters per second to provide a line-of-sight motion of 10 meters per second, resulting in a Doppler offset of about 2 MHz.

3.2.2 BACKSCATTER MEASUREMENTS

Measurements of the atmospheric backscatter coefficient were accomplished by comparing the return from the atmosphere with the return from a known calibrated target. It can be shown that the signal-to-noise ratio for a target such as a belt sander, when the beam is focused to a spot smaller than the size of the belt, is given by

$$SNR_{CAL} = \frac{\eta P}{h\nu B} \frac{(0.4)\ \pi D^2}{4\ f^2} \rho(\pi) \quad ,$$

where η is overall system efficiency,

P is laser power,

$h\nu$ is energy of a photon at optical frequency,

B is measurement bandwidth,

D is telescope diameter,

f is focal range of the system which is also range to target, and

$\rho(\pi)$ is target reflectivity.

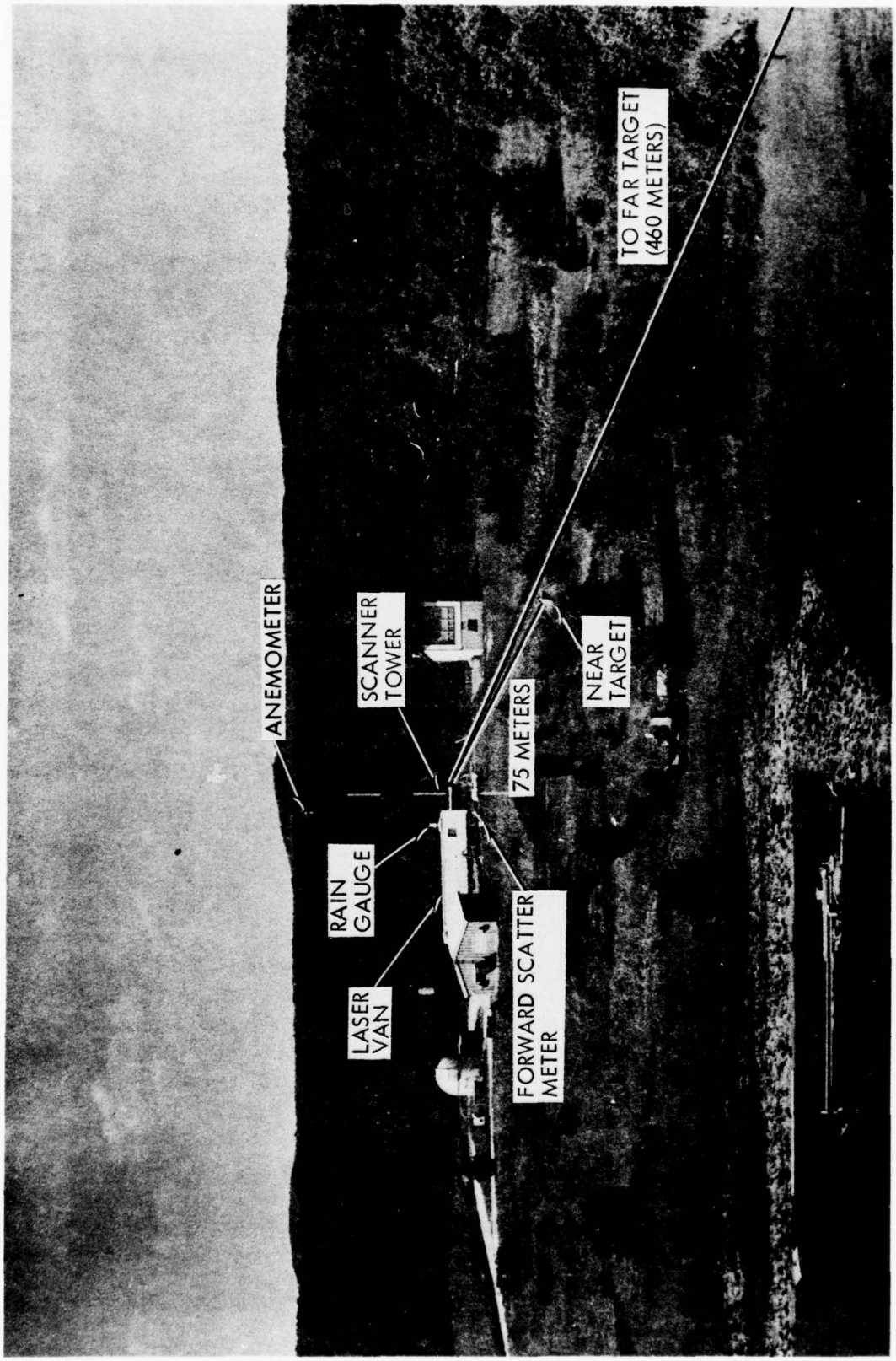

Figure 7. Laser Test Range at Raytheon's Sudbury Laboratories.

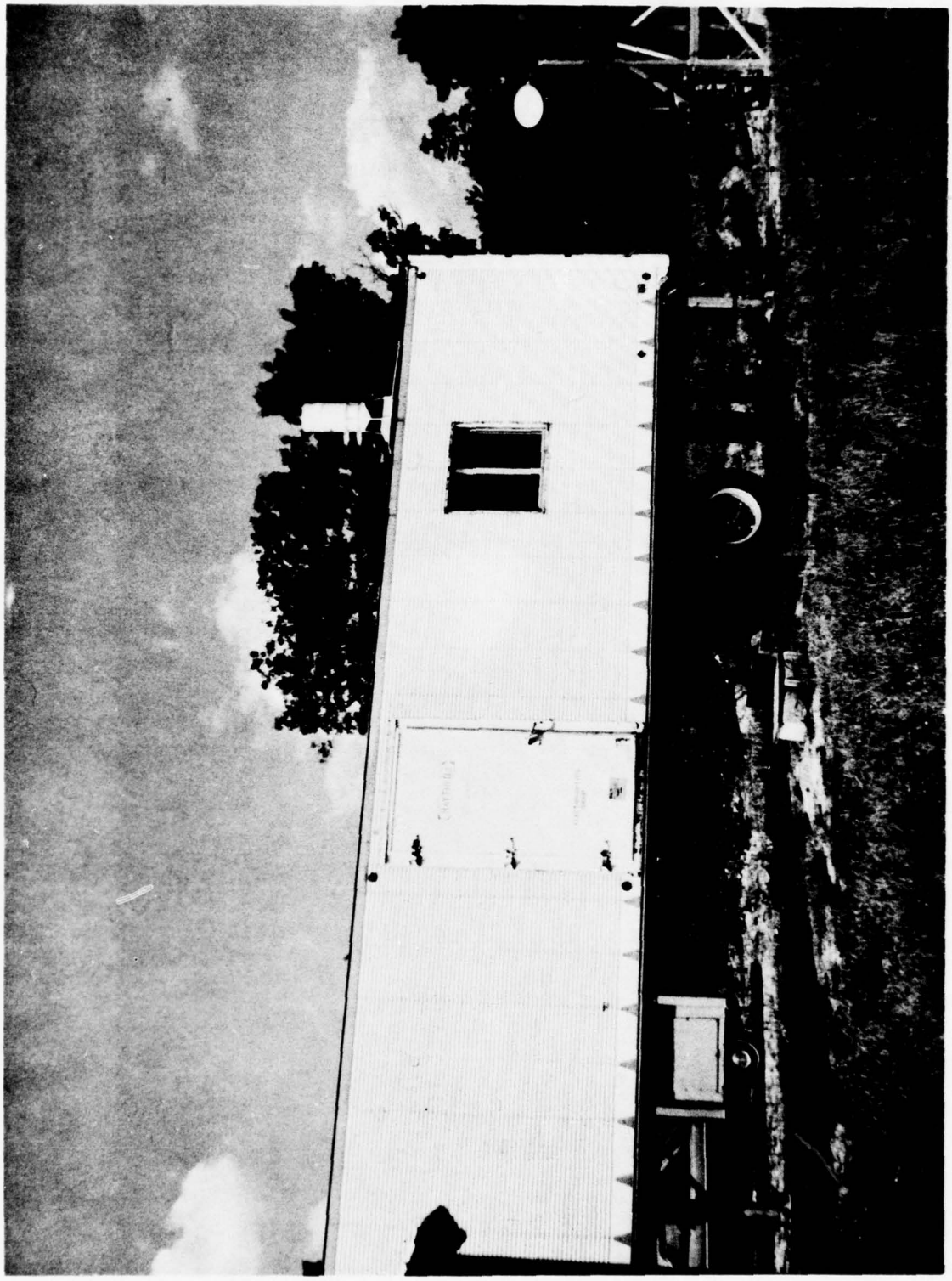

Figure 8. LASER SYSTEM VAN

The equation is valid for focal ranges much less than the far field distance. The far field of a one-foot optical system is approximately 7 kilometers, and the focal range used in this measurement is approximately 75 meters. The reflectivity, $\rho(\pi)$, is the amount of power backscattered per unit solid angle per unit of incident power. The signal-to-noise ratio in an atmospheric measurement with a focused system is given by the following equation,

$$SNR_{ATM} = \frac{\eta P}{h\nu B} \pi\lambda\beta(\pi),$$

where λ is optical wavelength, and

$\beta(\pi)$ is atmospheric nackscatter coefficient.

The backscatter coefficient, $\beta(\pi)$, here is defined as the amount of power backscattered per unit solid angle per unit of incident power per unit thickness of target.

By making the two measurements described above and determining the ratio of the two signal-to-noise measurements, it is possible to determine the atmospheric backscatter coefficient if the reflectivity of the hard target and the geometric parameters of the system are known. Specifically, the backscatter coefficient is obtained by the following equation,

$$\beta(\pi) = \frac{0.4\ \pi D^2}{4\ f^2}\ \rho(\pi)\ \frac{SNR_{ATM}}{SNR_{CAL}}\ .$$

Measurement of the atmospheric backscatter coefficient was accomplished by making the measurements indicated above. First, the laser beam was directed toward a target at 75 meters. The secondary position on the telescope was adjusted to maximize the signal received from this target, and a signal-to-noise ratio measurement was made. Then, the laser beam was directed to a point in space slightly above the target, and an atmospheric signal-to-noise ratio measurement was made.

A potential difficulty exists when the wind field in the focal volume is sufficiently turbulent that the spread in velocity within this volume is larger than that associated with the measurement bandwidth. In this case, the measured backscatter coefficient will be lower than the correct value. In general, it was found that a 100-kHz bandwidth was adequate for most of the atmospheric backscatter coefficients measurements. There were, however, days on which the spectral width of the atmospheric return was as large as 200 to 300 kHz.

3.2.3 ATTENUATION MEASUREMENTS

Measurement of the atmospheric attenuation coefficient is most directly accomplished by measuring the signal-to-noise ratios from two hard targets at different ranges. In the near field, the beam is collimated, and the signal-to-noise ratio from a hard target, such as the belt sander, is independent of range in the absence of atmospheric effects. Specifically, the signal-to-noise ratio is given by the following equation,

$$SNR_{CAL} = \frac{\eta P}{h\nu B} \frac{4\lambda^2}{\pi D^2} \rho(\pi) \quad e^{-2\alpha R} ,$$

where α is attenuation coefficient, and

R is range.

In this case, measurement of the atmospheric attenuation coefficient is particularly simple, requiring only measurement of the signal-to-noise ratio from two targets at different ranges in the near field, using a collimated beam, and knowledge of the range difference between the two targets. The actual experimental configuration is constrained by several considerations. It is important that the baseline length be carefully chosen, that the target be identical, and that the laser system performance be stable.

The length of the baseline for these measurements is an extremely significant parameter which must be carefully determined before setting up the system. Too short a baseline will not permit a sufficient attenuation to occur for accurate loss measurements to be made. On the other hand, a long baseline will magnify the effects of rainfall inhomogeneities, and will make the effect of atmospheric turbulence on the signal-to-noise ratio more important. It should be noted that the expression above for the signal-to-noise ratio does not include the effects of turbulence. For even longer ranges, the laser beam will begin to diverge due to diffraction effects, and the appropriate signal-to-noise ratio expression must then include the $1/R^2$ effects which occur in the far field. A satisfactory compromise was made by placing the far target at 460 meters from the system and the near target at 75 meters from the system as shown in Figure 7. This provided a roundtrip path-length difference between the targets of approximately 0.77 kilometer. Thus, an overall attenuation of 1 dB was obtained when the atmospheric attenuation coefficient was 1.3 dB per kilometer.

The target reflectivity was controlled by using sand belts which had been selected for sandpaper grade, and had been previously calibrated in the laboratory. Reflectivity is affected by humidity, and water directly on the belt can cause several dB of signal change. Reflectivities of the two belts were measured to be within 1 dB provided that water was prevented from accumulating on the belts. Protective housings were provided to prevent the accumulation of rain water on the belts. Some of the early measurements were made with the near target housed in a tent which did not completely protect it from rain water. The later measurements were made with both targets completely enclosed in wood shelters.

Laser system changes may occur as the temperature changes or as adjustments are made on the laser system. To minimize these changes, several precautions were taken. The telescope was adjusted to produce a collimated beam,and was not changed between the two measurements. Measurement of the signal from the far target is more difficult since it requires careful alignment of the beam on the target. Since may take a substantial amount of time, this measurement was made first. Then, after a reliable signal-to-noise ratio had been obtained, the beam was transferred quickly to the near target. This change could be accomplished in a period of less than 15 seconds. Additionally, the laser and van temperature were monitored to maximize stability of operation.

On clear days, it was verified that the signal-to-noise ratios of the two targets were equal to within 1 dB. This is estimated to be within the accuracy of the measurement technique.

3.2.4 METEOROLOGICAL DATA

The attenuation and backscatter data obtained as outlined above must be correlated with meteorological data to determine the laser system performance in adverse weather conditions. Equipment was available at various times during the program to monitor wind velocity, temperature, relative humidity, barometric pressure, visibility, rainfall rate, and particle size distributions.

The wind velocity was monitored with a three-axis Gill anemometer consisting of three propellers oriented in the northern, western, and vertical directions. These propellers were connected to generators which produced a direct current voltage proportional to the propeller speed, with the sign indicating the direction of motion. Wind velocities up to 50 knots could be read using these devices, and the three-dimensional wind vector could be obtained.

Temperature and relative humidity were measured using a Fischer sling psychrometer. Wet and dry bulb temperatures were obtained, and relative humidity was computed using appropriate tables.

Visibility was measured using an EG&G Model 207 forward-scatter visibility meter which was capable of measuring visibilities less than 20,000 feet. The baseline for this instrument was 4 feet.

The rainfall rate was measured with a Belfort Model 6069A rate of rainfall transmitter. This device used an inclined trough, the sides of which were plates of a capacitor connected to a capacitance bridge, to develop a DC voltage related to the rainfall rate. Calibration data for the instrument were available.

The meteorological data were summarized on datum log sheets along with the attenuation and backscatter measurements.

3.3 RESULTS

3.3.1 BACKSCATTER MEASUREMENTS

Backscatter measurements were made in both clear air and adverse weather. The backscatter coefficient is extremely variable, fluctuating over more than one order of magnitude in clear air. These fluctuations may take place over a comparatively short time span. Figure 9 shows the distribution of backscatter coefficients measured in clear air. The plotted datum points show the fraction of the total number of measurements which yielded backscatter coefficients of the indicated value within 0.5×10^{-8} m^{-1} sr^{-1} in clear air. The average backscatter coefficient is 3.3×10^{-8} m^{-1} sr^{-1}. The minimum backscatter coefficient measured was 0.5×10^{-8}, and the maximum was 10×10^{-8}.

The backscatter coefficient does not increase significantly in rain. This is partly because of the low backscatter coefficient of water and partly because the probability of at least one raindrop being in the focal volume is very small in light to moderate rainfall. The backscatter coefficient is plotted as a function of rainfall rate in Figure 10. Again, there is more than one order-of-magnitude variation in backscatter coefficient at low rainfall rates. An increase in backscatter coefficient is observed from approximately

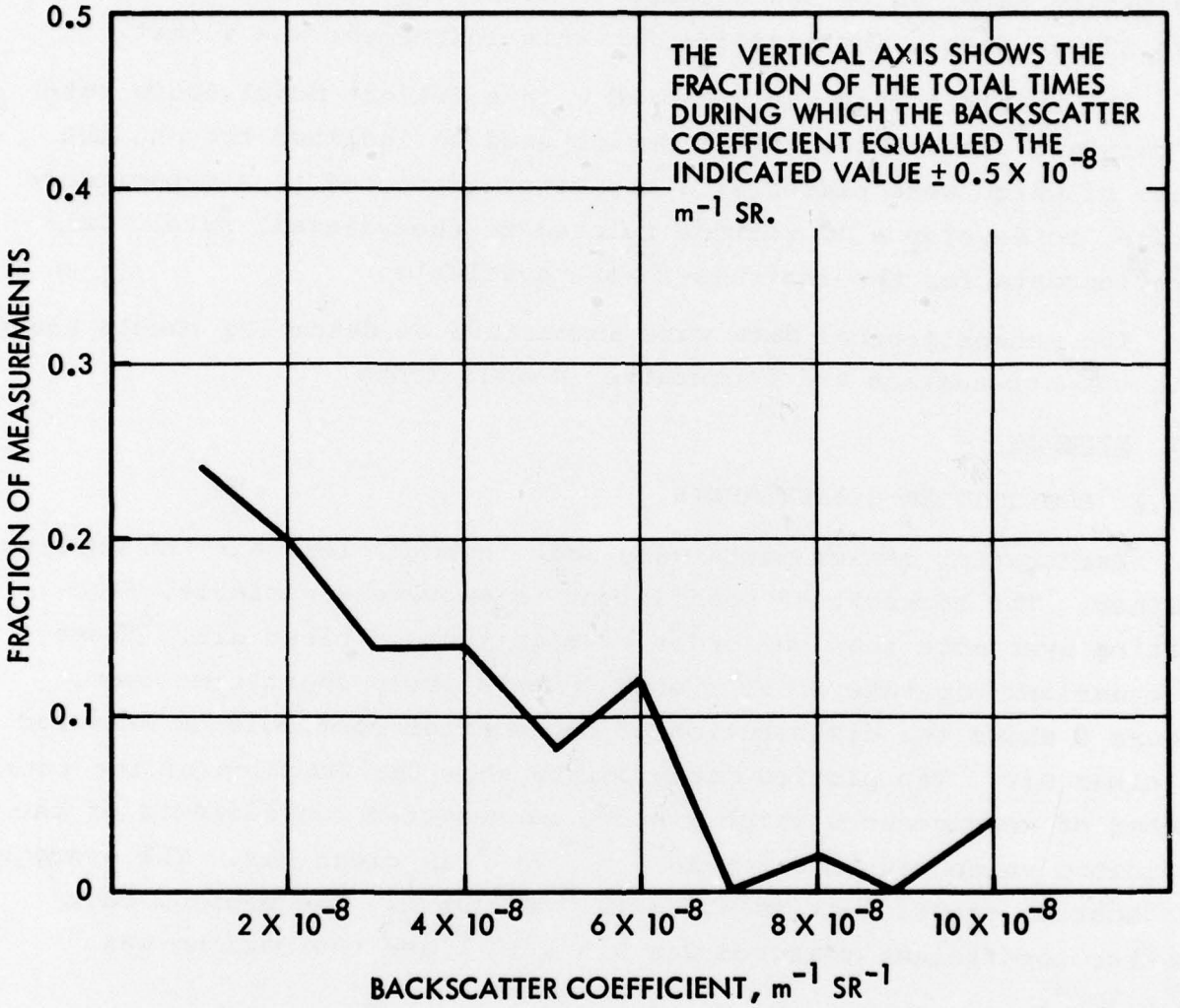

Figure 9. DISTRIBUTION OF BACKSCATTER COEFFICIENTS IN CLEAR AIR (49 Measurements)

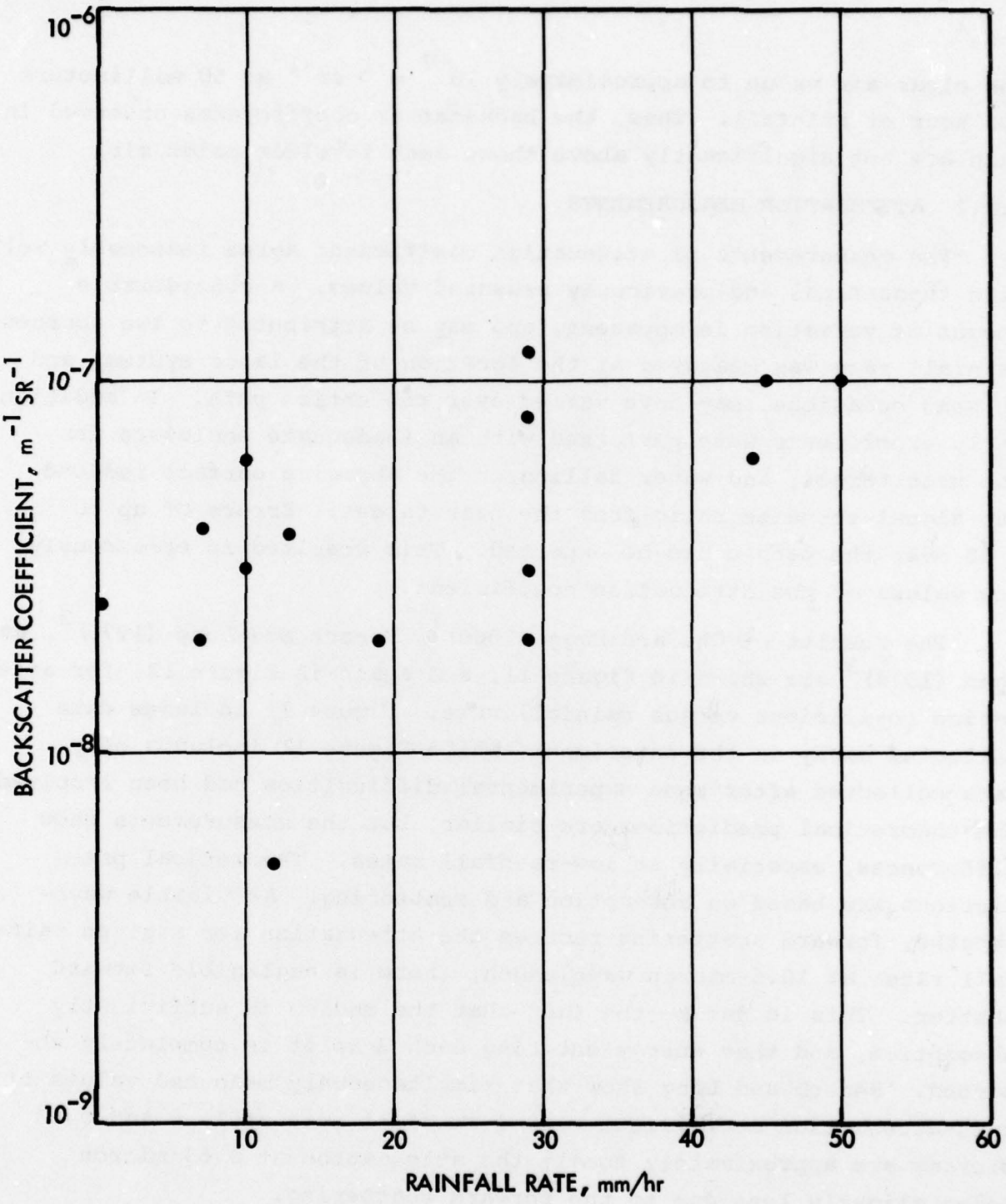

Figure 10. BACKSCATTER COEFFICIENT IN RAIN

the clear-air value to approximately 10^{-7} m^{-1} sr^{-1} at 50 millimeters per hour of rainfall. Thus, the backscatter coefficients observed in rain are not significantly above those seen in clear moist air.

3.3.2 ATTENUATION MEASUREMENTS

The measurements of attenuation coefficient agree reasonably well with theoretical and previously measured values. A considerable amount of variation is apparent, and may be attributed to two sources. Rainfall rate was measured at the location of the laser system, and on some occasions, may have varied over the entire path. In addition, early experiments were performed with an inadequate enclosure for the near target, and water falling on the abrasive surface reduced the signal-to-noise ratio from the near target. Errors of up to 6 dB over the path could be expected. This resulted in erroneously low values of the attenuation coefficient.

The results of Chu and Hogg (1968)[1], Rensch and Long (1970)[2], and Chen (1974)[3] are shown in Figure 11, and again in Figure 12, for attenuation coefficient versus rainfall rate. Figure 11 includes data collected early in the experiment, while Figure 12 includes only data collected after some experimental difficulties had been resolved. The theoretical predictions are similar, but the measurements show differences, especially at low-rainfall rates. Theoretical predictions are based on absorption and scattering. At visible wavelengths, forward scattering reduces the attenuation for a given rainfall rate; at 10.6-micron wavelength, there is negligible forward scatter. This is due to the fact that the medium is sufficiently absorptive, and that energy entering each droplet is completely absorbed. Rensch and Long show that simultaneously measured values of rain-attenuation coefficient versus rainfall rate at 10.6 and 0.63 microns are approximately equal; the attenuation at 0.63 micron being slightly less due to the forward scattering.

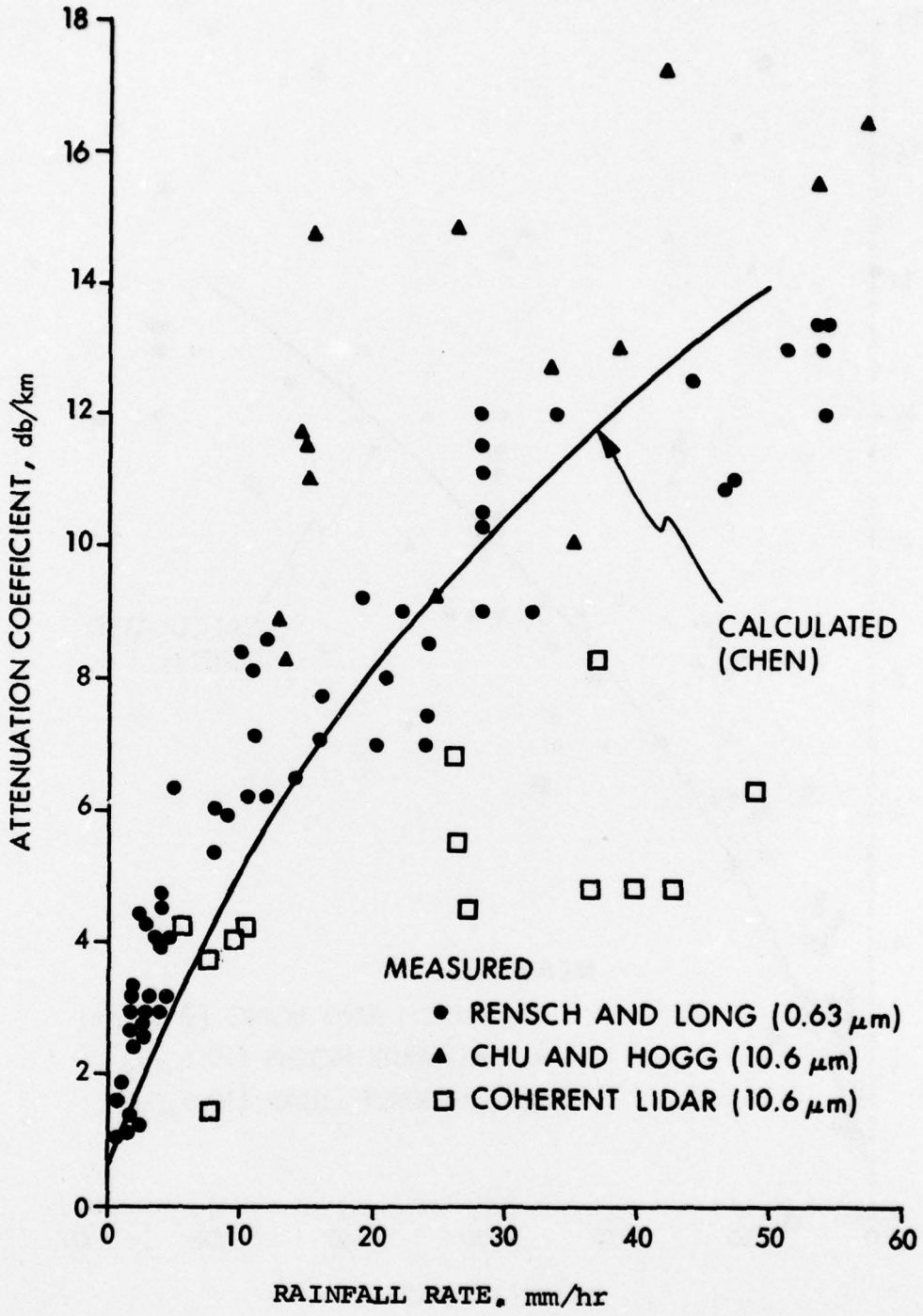

Figure 11. MEASURED AND CALCULATED ATTENUATION COEFFICIENT VERSUS RAINFALL RATE FOR ALL TESTS

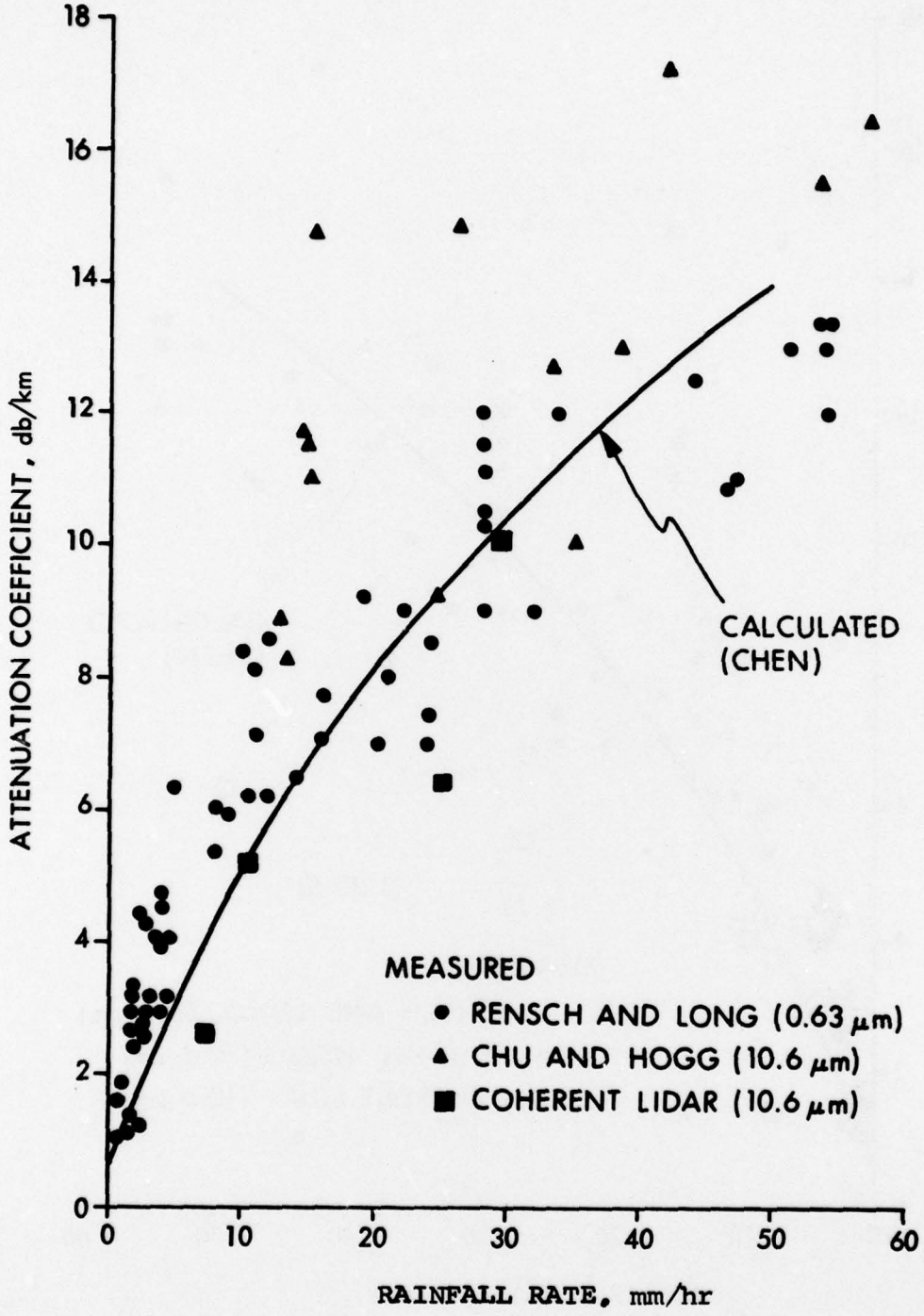

Figure 12. MEASURED AND CALCULATED ATTENUATION COEFFICIENT VERSUS RAINFALL RATE FOR SELECTED DATA

Due to the inadequate housing of the near belt sander, as was pointed out above, some of the datum points may be erroneously low in attenuation coefficient. Therefore, the datum points taken since the new target housing was installed have been shown separately in Figure 12. It is obvious that some of the early datum points (Figure 11) are in substantial disagreement with the expected values. Also, most of these disagreements occur at high-rainfall rates where it would be possible for a substantial amount of water to be present on the belt.

It should be noted that the later results agree well with the theoretical predictions, and do not exhibit the high attenuations at low-rainfall rates measured by Chu and Hogg. These measurements were obtained by a one-way transmission measurement, where it is difficult to separate the effects of beam motion and pure attenuation. We believe that the experimental procedure used here gives a more accurate measure of the attenuation experienced by a Lidar beam which backscatters off rain and aerosols in the atmosphere.

4. CONCLUSIONS

It may be concluded that a successful set of techniques has been developed for measuring backscatter and attenuation coefficients using a coherent CO_2 laser-Doppler velocimeter. The backscatter coefficients measured at Sudbury, Massachusetts, average approximately 3×10^{-8} m^{-1} sr^{-1} in clear air, and usually show an increase in adverse weather. In all types of weather, there appears to be somewhat more than due order-of-magnitude variation in the backscatter coefficient. Attenuation coefficients in rain agree well with anticipated results based on theoretical analyses and previous experimental measurements.

The SAW delay-line processor has been successfully integrated into the system, and appropriate software has been developed to determine the three components of the wind-velocity vector at a given altitude. All the necessary algorithms and displays are available to perform these calculations in real time.

5. REFERENCES

1. Chu,T.S., and Hogg,D.C., "Effects of Precipitation on Propagation at 0.63, 3.5, and 10.6 Microns", Bell System Technical Journal, No. 5 (1968).

2. Rensch,D.G., and Long,R.K., "Comparative Studies of Extinction and Backscattering by Aerosols, Fog and Rain at 10.6 Microns and 0.63 Microns", Applied Optics, Vol. 9, No. 7 (1970).

3. Chen,C.C., "A Correction for Middleton's Visibility and Infrared-Radiation Extinction Coefficient Due to Rain", Rand Corporation, R-1523-PR (1974).

APPENDIX---REPORT ON NEW TECHNOLOGY

There are no subject inventions to report under this contract. However, a new technique has been developed, which we believe to be an improvement over previous methods, for measuring performance of a CO_2 system in adverse weather. The advantages of the technique are that it is a direct measurement, and that it provides a nearly simultaneous reference measurement at close range. The two measurements are anticipated to yield the same signal in the absence of attenuation, and no system changes are required between the measurements. Thus, the two measurements provide a reliable measurement of the system performance in adverse weather. Relevant pages of the report are 20 through 22.

TABLE 1

Historical Highlights of CO_2 Lasers in Atmospheric Wind Research

1964 - First laser action observed in CO_2 gas.

1967 - First successful flight test of an optical homodyne CO_2 laser system.

1968 - First successful remote measurement of atmospheric wind with an optical homodyne CO_2 laser system.

1968 - First successful remote measurement of aircraft wake vortices with an optical homodyne CO_2 laser system. First successful field CO_2 laser Doppler MTI target imaging.

1970 - Demonstrated the feasibility of a pulsed Doppler CO_2 laser transmitter to be used for atmospheric turbulence detection.

1971 - First successful field measurement of hurricane-strength winds with a CO_2 laser homodyne system.

1971 - Demonstrated pulse Doppler CO_2 laser radar return over a two-mile path.

1972 - First successful flight test of a pulse Doppler CO_2 laser radar.

1973 - High quality images of moving Doppler targets with a CO_2 coherent detection Doppler imaging system.

1974 - First tracking of aircraft trailing vortices.

1974 - First development model of a coherent Doppler imaging system for a moving target to be carried in a remotely piloted vehicle.

1974 - First precision measurements of effluent from smoke stack scanning and velocity and space.

1976 - Development of the first helicopter remote wind sensor to be used as a fire control adjunct for free flight munitions.

1977 - Development of lightweight, man-portable 10.6 micron laser range finders.

1977 - Development of CW and Pulse Hybrid TEA Wind Shear system.

1977 - First remote measurement of thunderstorms from a ground based CO_2 laser sensor.